

Effects of Molecular Orientation on Surface-Enhanced Vibrational Spectroscopies

**Alicia M. Tripp, McNair Scholar
The Pennsylvania State University**

**McNair Faculty Research Advisor:
Lasse Jensen, Ph.D.
Associate Professor of Chemistry
Department of Chemistry
The Eberly College of Science
The Pennsylvania State University**

ABSTRACT

Both surface-enhanced Raman spectroscopy (SERS) and surface-enhanced hyper-Raman spectroscopy (SEHRS) allow for an increased spectral signal from molecules oriented on or near the surface of a metal nanoparticle. It is important to understand how the orientation of a molecule affects its enhanced spectra. In this work, electronic structure simulations were combined with the dressed-tensor formalism to simulate SERS and SEHRS spectra of a water molecule and a benzene molecule on the surface of or in the vicinity of an Ag nanoparticle. Through the simulations, it is found that the distance between the water molecule and the nanoparticle, whether ω was on resonance, and the inclusion or exclusion of field gradient effects impact the enhancement of the SERS and SEHRS spectra. It is also shown that rotational motions of a water molecule or a benzene molecule near a nanoparticle's surface influence the SERS and SEHRS spectrum observed as well.

INTRODUCTION

Raman is a vibrational spectroscopy that can be used to get information about the structure of molecules and how they behave in their environment under certain conditions.^{1,2} The observation of a molecule through these spectroscopies is dependent on the detection of frequencies that correspond to a molecule's normal modes. A normal mode is the synchronous motion of atoms or groups of atoms in a molecule that are excited without also causing the excitation of any other normal modes and the translation or rotation of the molecule. In order for a normal mode of a molecule to be observed in Raman spectroscopies, it must be Raman active, which requires a vibrational motion to occur with a change in polarizability.²

If a molecule's modes are Raman active, then a spectrum can be observed. In the two photon process of Raman spectroscopy, the incident photon can either scatter at a frequency or wavelength equal to (Rayleigh), less than (Stokes), or more than (anti-Stokes) its original frequency upon collision with a molecule. Stokes and anti-Stokes are the two types of Raman scattering that can be observed in Raman spectra.² Hyper-Raman spectroscopy is the nonlinear

version of Raman. Hyper-Raman spectroscopy can give complementary information to Raman, but instead of a two photon process, hyper-Raman utilizes three photons, such that there are two photons with the wavelength ω causing excitation, and then a single photon is scattered with a wavelength of $2\omega'$. The corresponding hyper-Raman line can be observed at the wavelength equal to the difference between the sum of the two incident photon energies and that of the single scattered photon.³

Unlike normal Raman and hyper-Raman spectroscopies, SERS and SEHRS require the use of metal nanostructures. Metal nanoparticles are used to enhance the signal because Raman and hyper-Raman are weak processes. Both the interactions between light and molecules and those between light and metal nanostructures must be considered in order to understand SERS and SEHRS. The light-metal interactions involved with these metal nanostructures can be explained through the concept of surface plasmon resonance (SPR).⁴

SPR is a coherent oscillation of the surface conduction electrons excited by EM radiation. Materials with a negative real and small positive imaginary dielectric constant are capable of supporting a SPR. Plasmonics involves the study of the SPR light-matter interactions, and surface-enhanced spectroscopies are among the array of its applications.⁵ Plasmonic metal nanostructures allow for the enhancement of the spectroscopies of molecules that are in contact with their surfaces.⁶ Thus, with the incorporation of a plasmonic nanoparticle (NP), enhanced Raman or hyper-Raman spectra of molecules oriented on or near the surface of such a NP is possible through SERS and SEHRS.⁷

The NP's strong local electric field allows for the possibility of single-molecule vibrational spectroscopy, and the spectral enhancement of the linear Raman and the nonlinear hyper-Raman vibrational spectroscopies is orders of magnitude greater than if they were not surface-enhanced by the use of metal nanostructures. These spectroscopic enhancements provide intensified signals and thus aid in the interpretation of a molecule's vibrational spectra. It is understood that the enhancement of the vibrational signal comes from a combination the electromagnetic (EM) mechanism and the chemical mechanism (CM). The EM mechanism occurs because of the strong local electric field at the NP surface caused by plasmon resonance, and the CM involves all of the other surface-molecule interactions.⁶

The majority of the enhancement is through the EM mechanism contribution, which is thought to enhance the signals by $|E^{loc}|^4$ for SERS, where E^{loc} is the local electric field the molecule experiences.⁸ The CM, however, does not contribute much to the total spectral enhancement. For SEHRS, the EM mechanism contribution to the enhancement coefficient is roughly scaled to $|E^{loc}|^6$. With the use of the dressed-tensor formalism, the EM mechanism of SERS and SEHRS can be understood and the incorporation of molecular orientation and field gradient (FG) effects in the simulated spectra is possible as well. When FG effects are included in calculation, then the molecule experiences an inhomogeneous local electric field, whereas if FG effects are not included, then the local electric field is homogeneous.⁶

It is important to understand how both field gradient effects and the orientation of a molecule affect its enhanced spectra. In this paper, a combination of electronic structure simulations and

the dressed-tensor formalism was used to simulate the SERS and SEHRS spectra of a water molecule and a benzene molecule on the surface of or in the vicinity of a silver NP. Through the simulations, it is found that whether the incident wavelength was on resonance, the inclusion or exclusion of field gradient effects, and the distance between a molecule and the nanoparticle impact the enhancement of the spectra. It is also shown that the orientation of the molecule near a nanoparticle's surface influences the enhancement observed as well.

THEORY

The SERS intensity for any active normal mode can be written as $I^{SERS} \propto \left| \frac{\partial \alpha}{\partial Q} \right|^2 \times |E^{loc}|^4$,

where α is the dipole-dipole polarizability, Q is the normal mode coordinates for a particular vibration, and E^{loc} is the strong local electric field from the excited nanoparticle that the molecule experiences. Likewise, the SEHRS intensity can be written as $I^{SEHRS} \propto \left| \frac{\partial \beta}{\partial Q} \right|^2 \times |E^{loc}|^6$, where β is the hyperpolarizability. It can be said that for a small spherical metal nanoparticle, $E^{loc} \sim \frac{A}{d^3}$, where A is some constant and d is the distance between the center of mass of the nanoparticle to that of the molecule of interest. If this approximation for E^{loc} were to be inserted into the I^{SERS} and I^{SEHRS} equations previously discussed, it would be expected that the enhancement factors would scale to approximately the 12th power for SERS and the 18th power for SEHRS when investigating the distance dependence for water and the silver nanoparticle. This expectation is based upon no FG effects taken into account in the calculations. However, the inclusion of FG effects introduces other EM mechanisms, which change the predicted values of the enhancement factors. Evidence of this will be presented in this work.⁶

COMPUTATIONAL DETAILS

The Dressed-Tensors Formalism. The dressed-polarizability formalism was used for all SERS and SEHRS simulations of water and benzene. In this formalism, the molecular transition polarizabilities were dressed using electric dipole–dipole (α), dipole–quadrupole (A), and quadrupole–quadrupole (C) transition polarizabilities for water's three normal modes and benzene's thirty. The polarizabilities for these two molecules were rotated to match their corresponding orientation in the silver nanoparticle reference frame. The local field enhancement matrices, which involve the incident field direction and the resulting field (or gradient) directions, were assumed to be identical at both the incident and scattered frequencies. The electric field and field gradient for the nanoparticle were calculated based upon an isotropic sphere, using the experimental dielectric functions of silver with incident light wavelengths of 343 nm for water and for benzene in Raman and at both 343 nm and 686 nm for water and at 686 nm for benzene in hyper-Raman.⁹

Quantum Mechanical Calculations. A local version of the Amsterdam Density Functional (ADF) program package was used for all quantum mechanical calculations involved in this work. For the geometry optimization and normal mode calculations, the local-density approximation (LDA) exchange correlation (XC)-potential and the triple zeta with one polarization function

(TZP) Slater type basis set was used, and the 1s core was kept frozen for oxygen for water and the 1s core was also kept frozen for carbon for benzene. The harmonic approximation was used to analytically calculate the vibrational frequencies and normal modes for the molecules of interest.

The polarizabilities and other properties needed for the normal and dressed-tensor Raman and hyper-Raman frequency independent simulations were calculated using the similar basis set previously described for geometry optimization and normal mode calculations with the 1s core kept frozen for oxygen for water, and the 1s core kept frozen for carbon in benzene. Frequency independent α , A , and C tensors were calculated using the AOResponse module implemented in ADF. Numerical three-point differentiation with respect to the Cartesian normal mode vibrational displacements was used to calculate the tensor derivatives. No symmetry was included in these calculations.⁹

RESULTS AND DISCUSSION

Distance Effects on Spectral Enhancement Factors. The spectral enhancement factors were roughly estimated based upon the best fit line generated for the normalized scatter plot of the recorded intensities of each of water's three vibrational modes 1556 cm^{-1} , 3690 cm^{-1} , and 3794 cm^{-1} over each translation distance in Bohr. The relation used to generate these best fit lines was $I \propto \frac{A}{d^{-x}}$ where I is the intensity of an observed spectral normal mode, A is a constant, and d^{-x} is the distance between the center of mass of the nanoparticle to that of the water molecule raised to some enhancement factor x . Figure 1 is an example of a such a plot for one of the SERS cases, and the data for all generated plots is located in Table 1. From the collected data, it is clear that as the NP was translated farther away from the molecule, the intensities of the spectra decreased. This is likely due to the decrease in local field strength the molecule felt as it became more separated from the NP's surface. How rapid the intensity drop-off was as the molecule was moved from the surface of the NP outward determined the x value. The inclusion of FG effects increased the value of x in all SERS and SEHRS spectra. In most instances, the incident wavelength (ω) used in SEHRS calculations impacted the enhancement factor as well.

Table 1: The collected distance dependence data for all generated normalized scatter plots in SERS and SEHRS.

Vibrational Spectroscopy	SERS	SERS	SEHRS	SEHRS	SEHRS	SEHRS
Field Gradient Effect	No	Yes	No	No	Yes	Yes
Incident Wavelength	343 nm	343 nm	343 nm	686 nm	343 nm	686 nm
Enhancement Factor	$x = 12$	$x = 14$	$x = 16$	$x = 14$	$x = 22$	$x = 22$

For SERS without FG effects at ω on resonance at 343 nm, the enhancement factor x was equal to 12. With FG effects, this factor increased by two orders of magnitude, such that 14 was the enhancement factor. When SEHRS was analyzed at the same ω with FG effects, $x = 22$ whereas without FG effects, the enhancement factor was four orders of magnitude less at $x = 16$. For SEHRS with FG effects at an incident ω off resonance at 686 nm, $x = 22$ whereas without FG effects $x = 14$ which is eight orders of magnitude less.

Clearly, the increase in the magnitude of the enhancement factors in all SERS and SEHRS spectra indicates that the spectral intensities for the normal modes decreased at a faster drop-off rate with FG effects compared to without. It can be seen that for the hyper-Raman plots at both 343 nm and 686 nm incident light frequencies with FG effects, the enhancement factor was $x = 22$. Whether or not the incident wavelength was on resonance had no perceivable effect on enhancement between these two particular spectra. However, for the hyper-Raman plots at both $\omega = 343$ nm and 686 nm without FG effects, the enhancement factor was two orders of magnitude smaller for the off resonance incident wavelength 686 nm.

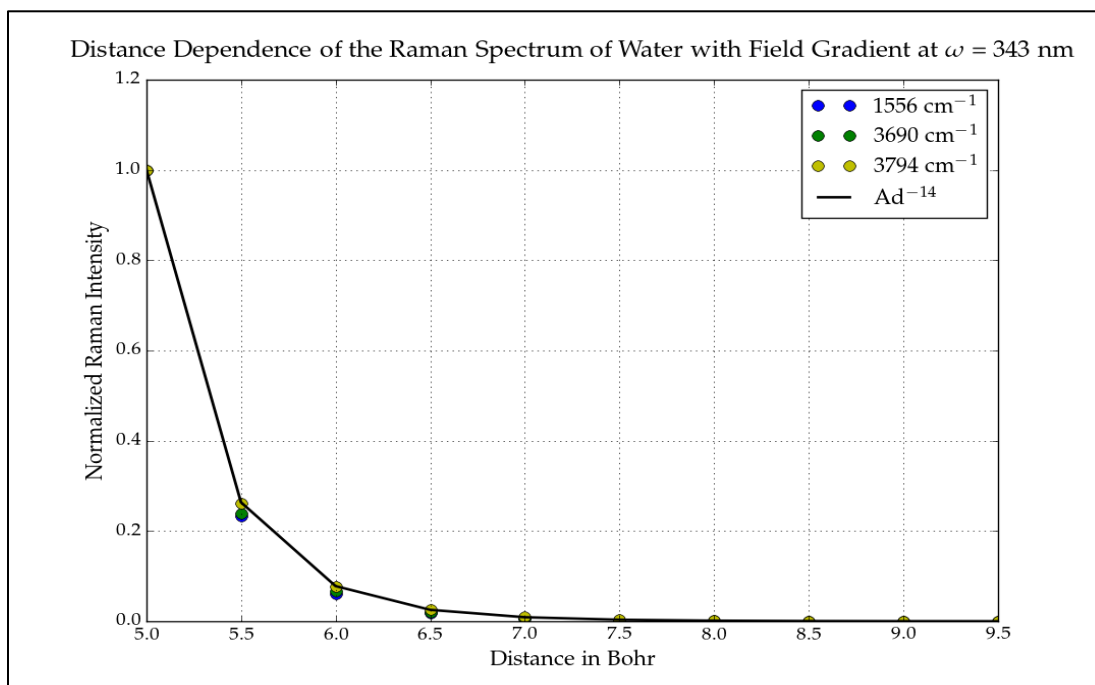


Figure 1: The normalized scatter plot of the SERS intensities of water observed as the molecule was translated farther from the nanoparticle. At distance 5.0 Bohr, the water molecule is at the surface of the silver NP of radius 5.0 Bohr. The enhancement factor here was 14.

Orientation Effects on the Enhancement of Spectra. The orientation effects were observed through the simulated normal and enhanced Raman and hyper-Raman spectra of both water and benzene by changing the orientation of the silver NP of radius 10 Bohr to be on either side of the molecule on the x, y, and z axes of the 3D Cartesian coordinate system. The water molecule's

coordinates lied in a y-z plane where the oxygen atom lied along the negative y-axis and one hydrogen atom was located in quadrant III and the other in IV. Benzene's coordinates were in a x-y plane where the origin was the center of the molecule. Field gradient effects were also included and excluded for the spectra generation.

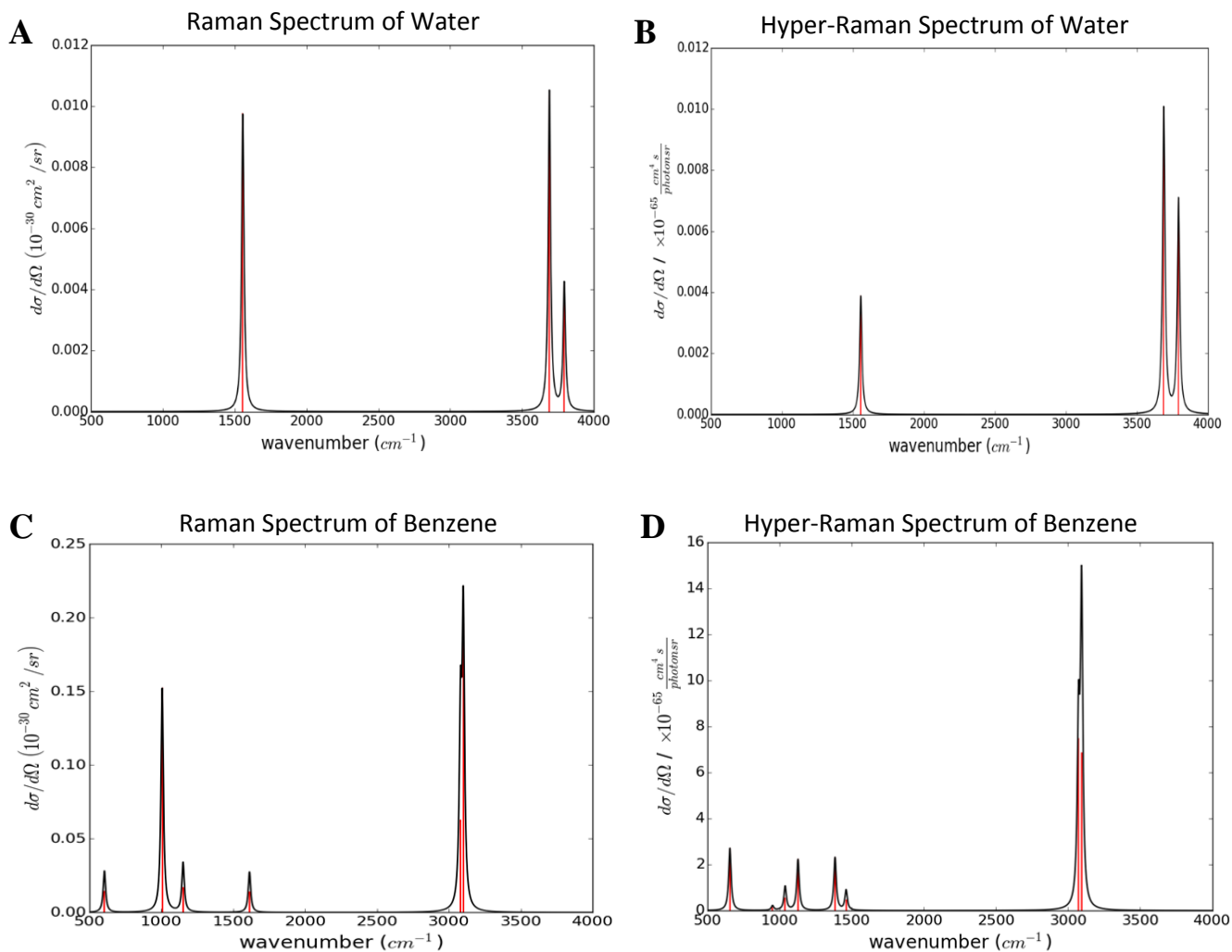


Figure 2: **A**, **B**, **C**, and **D** are the simulated normal Raman and hyper-Raman spectra of water and benzene. The scaled intensity for water's Raman and hyper-Raman's observed normal modes was $1.2 \times 10^{-32} \frac{cm^2}{sr}$ and $1.2 \times 10^{-67} \frac{cm^4 s}{photon sr}$ respectively. For benzene, the scaled intensity for Raman was $2.5 \times 10^{-31} \frac{cm^2}{sr}$ and for hyper-Raman it was $1.6 \times 10^{-64} \frac{cm^4 s}{photon sr}$.

It can be seen from **A** and **B** that water's three normal modes are present for both the normal Raman and hyper-Raman spectra, while **C** and **D** show that for benzene, there are normal modes observed in hyper-Raman that are not seen in Raman. The magnitude of the enhancements for all of the SERS and SEHRS spectra from Tables 2, 3, 4, and 5 were obtained from the comparison of the normal spectra's scaled intensities mentioned in the description of Figure 2 to that of the

surface-enhanced spectra. For water, all of the simulated SERS and SEHRS spectra had the same normal modes present as the normal spectra and only the intensities of these modes changed.

Table 2: The SERS enhancement data based upon the orientation of the NP to the water molecule and its normal Raman spectrum's intensity.

Axis of Rotation	X		Y		Z	
Field Gradient Effect	No	Yes	No	Yes	No	Yes
Enhancement	250	500	667	1.5×10^3	583	8 1.3×10^4

Table 3: The SEHRS enhancement data based upon the orientation of the NP to the water molecule and its normal hyper-Raman spectrum's intensity.

Axis of Rotation	X		Y		Z	
Field Gradient Effect	No	Yes	No	Yes	No	Yes
Enhancement	42	208	1.2×10^3	1.2×10^4	1.7×10^3	10 1.7×10^5

It can be clearly seen from Tables 2 and 3 that for both SERS and SEHRS, the orientation of the NP relative to the water molecule did not change the enhancement of the resulting spectra for the x and y axes. Whether the FG effects were included or not did change the enhancement observed, however. It can be said that the axis of rotation makes a difference for enhancement as well. The y-axis orientations had higher enhancements than the x-axis orientations. For the z-axis, there was a large difference in the enhancement for one orientation compared to the other for the SERS and SEHRS cases, including FG effects, and these values are emphasized in boxes in the tables.

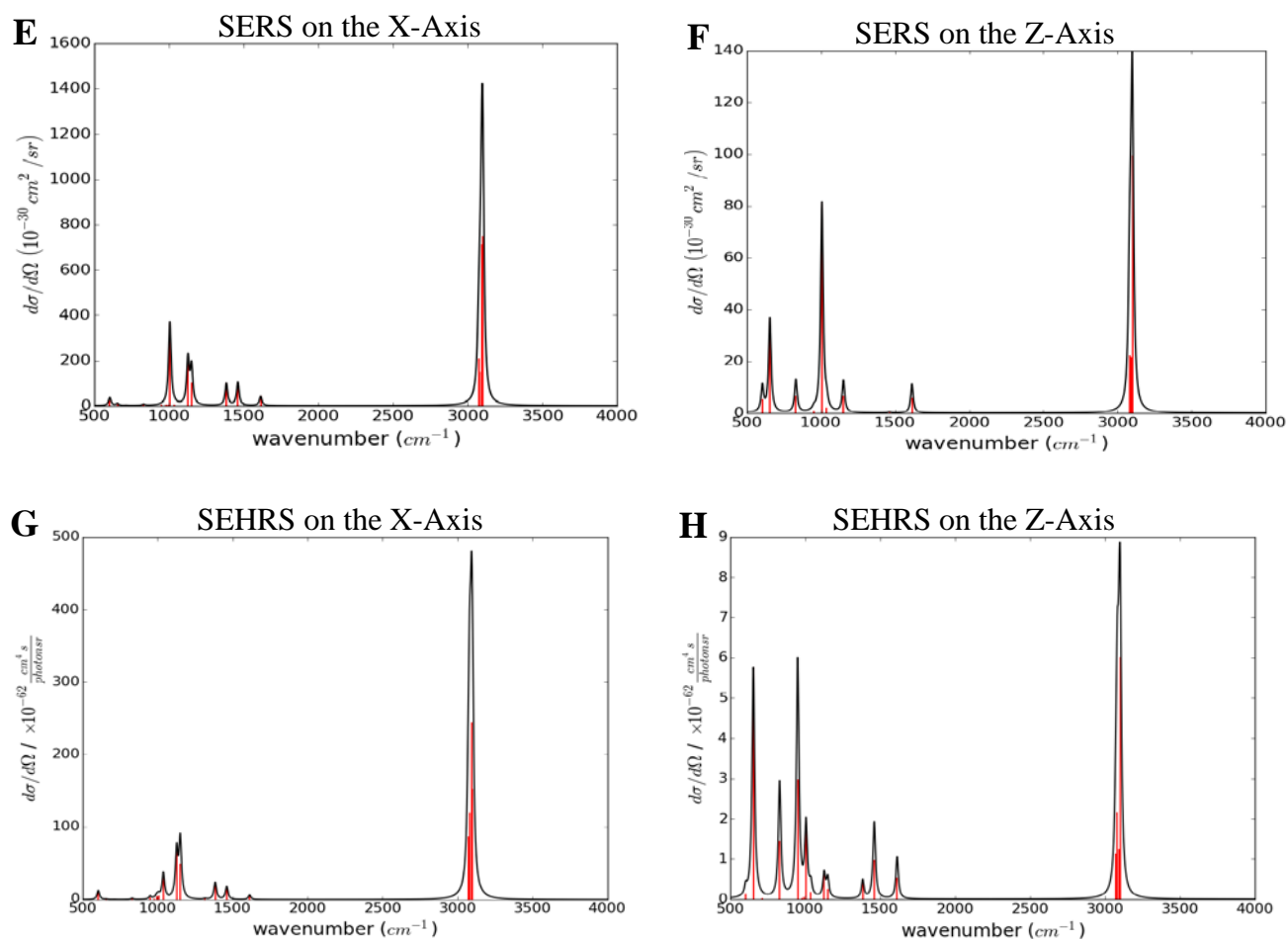


Figure 3: **E**, **F**, **G**, and **H** are the simulated SERS and SEHRS spectra of benzene for the x and z axes of rotation.

For benzene, the x and y-axis orientation spectra had the same observable modes and only the intensities of the peaks changed. However, it can be noted from Figure 3 that new modes were observed when comparing the x-axis spectra **E** and **G** to the z-axis spectra **F** and **H** for SERS and SEHRS as well as when comparing only **F** and **H**. This indicates that the orientation of the molecule as well as the method of spectroscopy can affect the normal modes that are able to be observed in spectra. Tables 3 and 4 provide the SERS and SEHRS enhancement data for benzene when compared to the normal spectrum's scaled intensities from **C** and **D** in Figure 2.

Table 4: The SEHRS enhancement data based upon the orientation of the NP to the benzene molecule and its normal Raman spectrum's intensity.

Axis of Rotation	X		Y		Z	
Field Gradient Effect	No	Yes	No	Yes	No	Yes
Enhancement	1,000	6.4×10^3	1,000	6.4×10^3	80	320
	480	4.0×10^3	480	4.8×10^3	320	560

Table 5: The SEHRS enhancement data based upon the orientation of the NP to the benzene molecule and its normal hyper-Raman spectrum's intensity.

Axis of Rotation	X		Y		Z	
Field Gradient Effect	No	Yes	No	Yes	No	Yes
Enhancement	156	1.6×10^4	188	1.9×10^4	125	562
	1.3×10^3	3.1×10^4	1.3×10^3	7.5×10^4	156	500

From Tables 4 and 5, it can be seen that for benzene the orientation does change the enhancement for all of the axes, not just for the z-axis with FG effects included like water. When the data from Tables 2, 3, 4 and 5 are considered, it is clear that for both water and benzene, the inclusion of FG effects leads to a larger spectral enhancement.

CONCLUSIONS

There are a few conclusions that can be made from all of the data and spectra presented in this work. From the distance dependence data, it is clear that the molecule of interest must be at the surface of the NP for the best enhancement to occur. As the molecule is translated farther from the surface of the NP, the strong local electric field becomes less of an influence on the molecule, and thus the enhancement of the spectra decreases. Distance dependence data from Table 1 supports the conclusion that including FG effects leads to a faster intensity drop off for observed spectra, which leads to an increase in enhancement. Also, Table 1 shows that the predicted values of the enhancement factors of 12 for SERS and 18 for SEHRS discussed in the **THEORY** section were not in agreement with the factors found through simulation. This

indicates that the inclusion of FG effects introduces other EM mechanisms, which can change these values. It is also seen from Table 1 that the incident wavelength exciting the molecule can affect the enhancement factor of SEHRS spectra. An ω on resonance with the excitation wavelength of the plasmonic NP had a larger enhancement factor and thus a larger spectral enhancement than an incident wavelength that was off resonance.

From the orientation data in Tables 2, 3, 4, and 5, it is clear that certain orientations provide larger enhancements. Thus orientation is an important factor to consider when attempting to detect molecules of interest. It can also be seen from **A, B, C, and D** from Figure 2 and **E, F, G, and H** from Figure 3 that there are normal modes observed in SEHRS spectra that are not seen in SERS spectra. Figure 3 also shows that orientation can have an influence on what normal modes are observed as well.

A final conclusion to be made is that molecules can be identified by their unique Raman spectrum. This can be said because for water, there were three distinct normal modes that were consistent in appearance through all spectra, thus water could be easily identified using a reference spectrum. Also, for benzene, the normal modes that consistently appear in the fingerprint region of 500-2,000 cm^{-1} could be used for identification.

Future work will include the simulation of the spectra of larger molecules using similar methodology that was used for water and benzene. Molecules such as naphthalene and anthracene would logically be the next two molecules of interest as they build off of benzene. Also, it would be interesting to use metal nanoparticles of different geometries other than just the small spherical model. The investigation of the spectral enhancements that arise from these other geometries and how they compare to previously collected data from the spherical model is certainly an interest for future work.

ACKNOWLEDGEMENTS

This work was supported by the Ronald E. McNair Post-Baccalaureate Achievement Program and The Eberly College of Science through The Pennsylvania State University.

LITERATURE CITED

1. Crouch, S., Holler, F., Skoog, A. *Principles of Instrumental Analysis*, 6th ed.; Cengage Learning: Belmont, 2007; pp 132-133.
2. Atkins, P., Paula, J. *Physical Chemistry: Thermodynamics, Structure, and Change*, 10th ed.; Oxford University Press: Oxford, 2014; pp 286-477.
3. Li W.H.; Li X.Y.; Yu N.T. Surface-enhanced hyper-Raman spectroscopy (SEHRS) and surface-enhanced Raman spectroscopy (SERS) studies of pyrazine and pyridine adsorbed on silver electrodes. *Chem. Phys. Lett.* **1998**, *305*, 303-310.

4. Schlücker, S. Surface-Enhanced Raman Spectroscopy: Concepts and Chemical Applications. *Angew. Chem. Int. Ed. Engl.* **2014**, *53*, 4756-4795.
5. Willets K.A.; Van Duyne R.P. Localized surface plasmon resonance spectroscopy and sensing. *Annu. Rev. Phys. Chem.* **2007**, *58*, 267–297
6. Dhabih C.V.; Zhongwei H.; Moore J.E.; Chen X.; Jensen L. Theory of Linear and Nonlinear Surface-Enhanced Vibrational Spectroscopies. *Annu. Rev. Phys. Chem.* **2016**, *67*, 23.1-23.24.
7. Kelley A.M. Hyper-Raman Scattering by Molecular Vibrations. *Annu. Rev. Phys. Chem.* **2010**, *61*, 41-61.
8. Dhabih C.V.; Chen X.; Jensen L. Simulating Ensemble-Averaged Surface-Enhanced Raman Scattering. *J. Phys. Chem. C.* **2016**.
9. Dhabih C.V.; Jensen L. Determining Molecular Orientation With Surface-Enhanced Raman Scattering Using Inhomogeneous Electric Fields. *J. Phys. Chem. C.* **2013**, *117*, 19622-19631.